Topological Phase Transitions in Zinc-Blende Semimetals Driven Exclusively by Electronic Temperature

Egor Trushin and Andreas Görling*
Lehrstuhl für Theoretische Chemie, Universität Erlangen-Nürnberg, Egerlandstr. 3, D-91058 Erlangen, Germany

(Received 27 June 2017; revised manuscript received 15 December 2017; published 4 April 2018)

We show that electronic phase transitions in zinc-blende semimetals with quadratic band touching (QBT) at the center of the Brillouin zone, like GaBi, InBi, or HgTe, can occur exclusively due to a change of the electronic temperature without the need to involve structural transformations or electron-phonon coupling. The commonly used Kohn-Sham density-functional methods based on local and semilocal density functionals employing the local density approximation (LDA) or generalized gradient approximations (GGAs), however, are not capable of describing such phenomena because they lack an intrinsic temperature dependence and account for temperature only via the occupation of bands, which essentially leads only to a shift of the Fermi level without changing the shape or topology of bands. Kohn-Sham methods using the exact temperature-dependent exchange potential, not to be confused with the Hartree-Fock exchange potential, on the other hand, describe such phase transitions. A simple modeling of correlation effects can be achieved by screening of the exchange. In the considered zinc-blende compounds the QBT is unstable at low temperatures and a transition to electronic states without QBT takes place. In the case of HgTe and GaBi Weyl points of type I and type II, respectively, emerge during the transitions. This demonstrates that Kohn-Sham methods can describe such topological phase transitions provided they are based on functionals more accurate than those within the LDA or GGA. Moreover, the electronic temperature is identified as a handle to tune topological materials.

DOI: 10.1103/PhysRevLett.120.146401

Topological insulators [1] and related materials attract enormous interest both for fundamental reasons and due to potential technical applications. Temperature is considered as a possible handle to control topological order and to induce topological phases. Furthermore, if temperature influences the topological nature of the electronic structure of a material this needs to be understood before a designing of technical devices can be envisioned. Reliable predictions of electronic properties of materials are obtained from first-principles methods that are typically based on the Kohn-Sham (KS) formalism of density-functional theory (DFT) [2,3]: so far, first-principles investigations of temperature effects of topological insulators and their phase transitions concentrated on the temperature dependence of phonon effects [4–7], i.e., electron-phonon coupling. Furthermore, topological phase transitions were obtained in DFT calculations mimicking temperature-driven structural transformation; see, e.g., Ref. [8]. We here show that temperature can lead to phase transitions in zinc-blende semimetals without taking into account phonons or structural transformations just via the direct effect on the electronic structure. That is, the electronic temperature alone can lead to phase transitions. In particular, we demonstrate that the quadratic band touching (QBT) at the center of the Brillouin zone of GaBi, InBi, and HgTe vanishes at low electronic temperature and a transition to another electronic state occurs. In GaBi and HgTe, moreover, Weyl points [9–12] emerge during the transitions.

The findings of this Letter thus point to a new mechanism for manipulating the topological nature of materials. Exploiting this mechanism opens up new opportunities in predicting and designing topological insulators and related material provided it can be reliably described. We show that this is not possible with the commonly used KS methods based on exchange-correlation functionals employing the local density approximation (LDA) or the generalized gradient approximation (GGA) [2,3]. The reason is that LDA or GGA functionals cannot take into account the intrinsic temperature dependence of exchange and correlation. Temperature is accounted for merely by the temperature dependence of the occupation of bands via the Fermi distribution function. As shown below this essentially leads only to a shift of the Fermi energy without changing the shape of the bands. We then demonstrate that KS methods with functionals going beyond the LDA or GGA can describe topological phase transitions caused by electronic temperature. More specifically the exact temperature-dependent KS exchange potential with its intrinsic temperature dependence is shown to describe temperature-driven qualitative changes of band structures including phase transitions. The exact nonzero-temperature KS exchange potential is a local multiplicative potential that must not be confused with the nonlocal Hartree-Fock exchange potential. In Ref. [13] the nonzero-temperature exact-exchange (EXX) KS approach is introduced. It is based on the

nonzero-temperature density-functional theory of Mermin [14]. The nonzero-temperature EXX approach generalizes the corresponding zero-temperature EXX method [15,16] and like the latter constructs the local multiplicative EXX potential via the optimized effective potential method [17,18]. In this Letter we combine the nonzero-temperature EXX approach with a treatment of spin-orbit interactions and noncollinear spin. The computational requirements of EXX KS methods including those for nonzero temperature [13,19] are roughly that of hybrid density-functional methods. A nonzero-temperature Hartree-Fock treatment of the effects considered here is not possible due to the artificially vanishing density of states at the Fermi level in the Hartree-Fock method.

Besides pointing to a new handle to design materials with topologically interesting electronic structures, the results of this work show that conventional LDA or GGA methods are not sufficient to describe temperature effects in such materials. A complete description requires the use of exchange-correlation functionals with intrinsic temperature dependence. The EXX method employed here represents a starting point to that end.

The EXX method treats exchange exactly but neglects correlation. To model the physical effect of correlation we replaced the electron-electron interaction $1/|\mathbf{r}-\mathbf{r}'|$ within the exchange by a screened one, that is, by $\exp[-\gamma|\mathbf{r}-\mathbf{r}'|]/|\mathbf{r}-\mathbf{r}'|$. While such a simple screening cannot be expected to yield highly accurate total energies, it is ideal to investigate how robust our findings are with respect to correlation effects because we can tune the latter by varying the parameter γ. All major effects, i.e., the transitions to magnetic phases, discussed in the manuscript for the pure EXX case remain present in the case of screening, even for quite large γ values of 0.3 corresponding to a screening of exchange by a factor of $1/e$ at a distance of 1.7 Å. See Supplemental Material (SM) [20], which includes Refs. [21–35], for details on the results obtained with screened exchange.

Our calculations were performed with the MCEXX program [36] based on norm-conserving pseudopotentials and plane-wave basis functions; see SM [20] for details. The implementation of the nonzero-temperature EXX approach in the MCEXX program is described in Ref. [13]. We sample the Brillouin zone with a regular Γ-point-centered grid of $8\times8\times8$ $\mathbf{k}$ points. The plane-wave cutoff was set to 60 a.u. for the one-electron KS functions and to 30 a.u. for the representation of the exchange potential and the response function. The calculations take into account noncollinear spin. Spin-orbit interactions are included via pseudopotentials [37] that were generated with the code of Ref. [38]. For In and Hg, the semicore d electrons are treated as valence electrons, whereas for other atoms only the energetically highest s and p electrons are included in the valence space. We use the experimental lattice parameter of 6.453 Å for HgTe [39] and lattice parameters of 6.457 and 6.853 Å for GaBi and InBi [40], respectively, which were optimized by density-functional calculations with the exchange-correlation functional of Perdew *et al.* [41]. In all cases the nuclear positions were kept fixed and only the electronic temperature was varied.

We tested how robust the observed effects due to nonzero electronic temperature are with respect to the effect of temperature on the nuclear degrees of freedom by repeating our calculations for modified lattice constants to model thermal expansion. No qualitative changes were observed; for details see SM [20].

Figure 1 displays the LDA and EXX band structures of GaBi. Both band structures are displayed twice: (i) in the usual way with respect to the Fermi level and (ii) with the energy of the QBT set to 0. In this second view changes of the form of bands due to temperature variation can easily be detected. Figure 1 clearly shows that the LDA band structures for all electronic temperatures exhibit almost exactly the same form even at a temperature of 10 000 K that does not make sense for a solid. The only effect of raising the electronic temperature is a shift of the Fermi energy. The form of EXX band structures, on the other hand, exhibits sizable changes with temperature. Note that the so-called Lifshitz transition, i.e., the change of the topology of the Fermi surface [42,43], occurs at $T\approx500$ K, when the two energetically lowest bands that are located above the Fermi energy at higher temperatures cross the Fermi level near the L point. In the LDA band structures this intersection is present at all temperatures, which represents a qualitatively different behavior.

Even stronger differences between LDA and EXX band structures manifest themselves at lower temperatures; see Fig. 2 and SM [20]. Within the EXX description, the electronic structure of GaBi is unstable towards a magnetic state. The QBT disappears and instead spin-polarized flat bands are formed in the vicinity of the original position of the QBT. The flattening of bands near the Γ point with the formation of an energy gap at the Γ point can possibly be interpreted as a Fermi condensation due to a van Hove singularity locally presented at the QBT [44,45]. After the phase transition, spin splittings of bands along the Γ–L path become very large and clearly visible in the band structure; see SM [20] for figures showing the magnitude of magnetization in real space. Note that even before the phase transition, noncollinear spin due to spin-orbit interactions leads to tiny splittings of bands that cannot be resolved at the scale of Fig. 1.

Further lowering of the temperature to 50 K leads to another phase transition to a second magnetic state with a Weyl point of type II [12] lying on the Γ–L path about 0.2 eV above the Fermi level; see Fig. 2. In a LDA description neither of the phase transitions occurs, and the band structure does not exhibit any changes when lowering the temperature except the mentioned shift of the Fermi level; see SM [20] for LDA band structures at low temperatures.

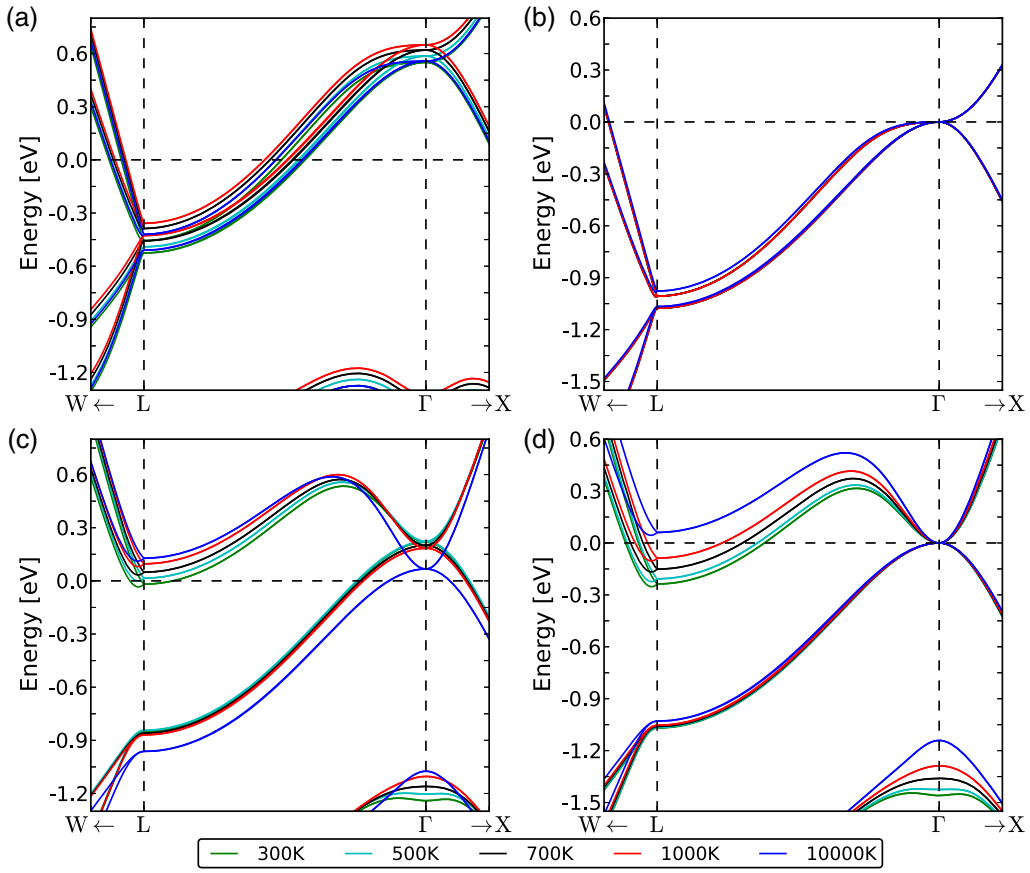

FIG. 1. Band structure of GaBi at various temperatures calculated within LDA [(a) and (b)] and EXX [(c) and (d)]. The zero point of the energy axis corresponds to the Fermi level [(a) and (c)] or the energetic position of the point of the quadratic band touching [(b) and (d)].

The electronic structure of InBi exhibits a similar behavior with temperature. Within EXX, the transition from the phase with QBT to the magnetic phase with flat bands and an energy gap at the Γ point occurs at about 500 K. A second phase transition at lower temperature is not found. Again no phase transitions occur within the LDA. See SM [20] for band structures of InBi.

HgTe exhibits a behavior distinct from that of GaBi and InBi. When the instability of the QBT occurs at $T \approx 500$ K, the electronic structure hosts a Weyl point of type I almost exactly at the Fermi level on the Γ–L path; see Fig. 3. If the temperature is further decreased then a small gap between the initially touching bands appears. For temperatures approaching 0 the size of the gap is about 5 meV. See

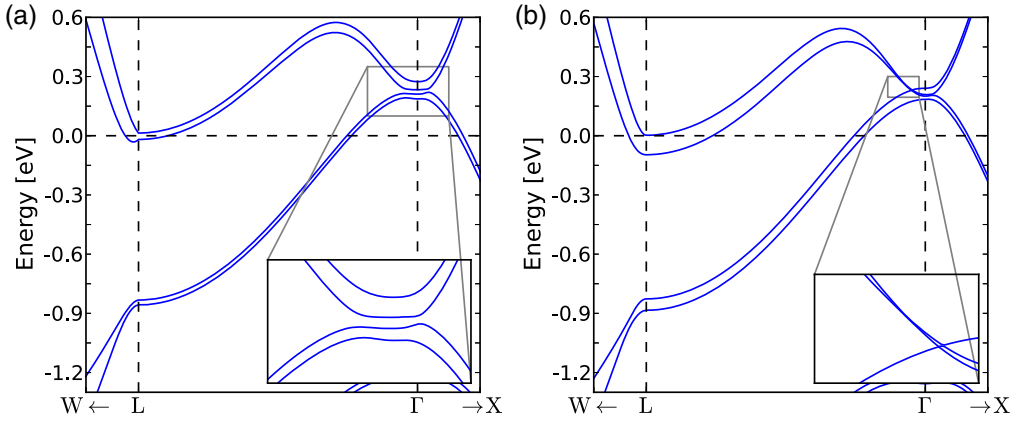

FIG. 2. Band structure of GaBi at 100 (a) and 50 K (b) calculated within EXX. The zero point of the energy axis corresponds to the Fermi level.

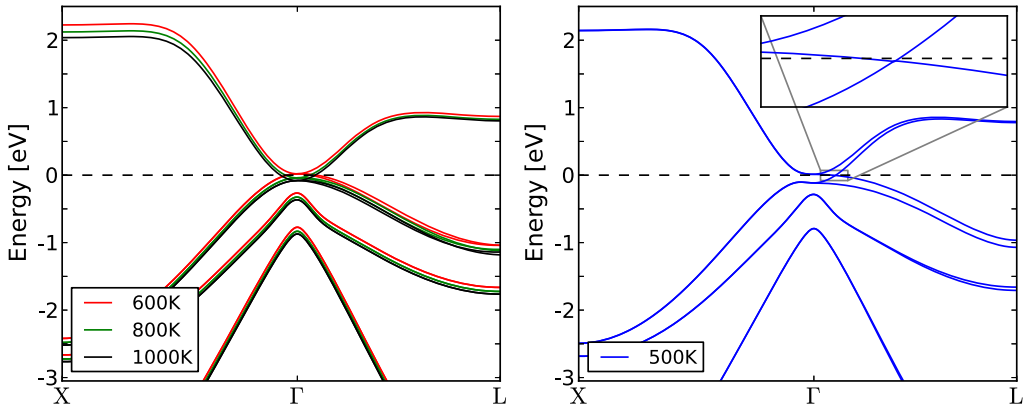

FIG. 3. Band structure of HgTe at various temperatures calculated within EXX. The zero point of the energy axis corresponds to the Fermi level.

SM [20], for the band structure at T = 5 K. Note that an analogous transition from an electronic state with QBT to a state with a Weyl point was found in Ref. [46] for $Pr_2Ir_2O_7$ in GGA + U calculations by increasing the value of the parameter U.

From the presented results, it is evident that proper nonzero-temperature density-functional calculations are required not only in the high-temperature regime, e.g., for warm dense matter [47], but also can be essential in the low- and room-temperature domain. In this work we showed that electronic phase transitions may be induced exclusively by changes of the electronic temperature. Additionally, this suggests, however, that temperature-driven phase transition due to electron-phonon coupling or due to temperature-induced structural changes may be coupled to or at least influenced by temperature effects in the electronic structure. Indeed, at low temperatures lattice dynamics is suppressed except for zero-point vibrations, whereas effects due to the electronic temperature were shown here to be present even at very low temperatures in some case and therefore should be taken into account whenever temperature effects are considered.

The vanishing of the QBT at low temperatures found in our EXX calculations supports speculations in the literature about possible low-temperature instabilities of QBTs in zinc-blende materials and certain pyrochlore iridates [46,48–50]. In our calculations two distinct situations after the breaking of the QBT are found, one with (HgTe, second transition in GaBi) and one without (first transition in GaBi, InBi) the appearance of Weyl nodes. The nondispersive flat bands formed in the latter case near the original position of the QBT are consistent with recent experimental results for $Nd_2Ir_2O_7$ [51].

We have concentrated on a comparison of LDA and EXX band structures. GGA band structures can be assumed to exhibit a similar temperature dependence as LDA band structures because GGA functionals like LDA functionals neglect any explicit temperature dependence of exchange and correlation. Indeed GGA band structures of GaBi and HgTe in Refs. [52,53] resemble the LDA band structures of this work.

In summary, we conclude that a proper nonzero-temperature extension of DFT is mandatory for a reliable and comprehensive description of temperature-driven physics in topological materials. The nonzero-temperature EXX approach of Ref. [13] employed in this work represents a first truly temperature-dependent KS method. A simple modeling of correlation effects by a screening of the exchange did not lead to qualitative changes. This suggests that previous experience in the zero-temperature case that exact exchange-only band structures typically are of good quality transfers to the nonzero-temperature regime. A future path to correlation functionals with explicit temperature dependence may be based on the adiabatic-connection fluctuation-dissipation theorem [54,55] or a proper nonzero temperature generalization thereof, starting perhaps with a nonzero-temperature generalization of the random phase approximation [56].

This work was supported by the German Science Foundation [Deutsche Forschungsgemeinschaft (DFG)] through the Cluster of Excellence "Engineering of Advanced Materials" [57].

*andreas.goerling@fau.de

[1] M. Z. Hasan and C. L. Kane, Rev. Mod. Phys. **82**, 3045 (2010).
[2] R. G. Parr and W. Yang, *Density-Functional Theory of Atoms and Molecules* (Oxford University Press, Oxford, 1989).
[3] R. M. Dreizler and E. K. U. Gross, *Density Functional Theory* (Springer, Heidelberg, 1990).
[4] I. Garate, Phys. Rev. Lett. **110**, 046402 (2013).
[5] K. Saha and I. Garate, Phys. Rev. B **89**, 205103 (2014).
[6] B. Monserrat and D. Vanderbilt, Phys. Rev. Lett. **117**, 226801 (2016).

[7] G. Antonius and S. G. Louie, Phys. Rev. Lett. **117**, 246401 (2016).
[8] S. Eremeev, I. Rusinov, P. Echenique, and E. Chulkov, Sci. Rep. **6** (2016).
[9] L. Balents, Physics **4**, 36 (2011).
[10] X. Wan, A. M. Turner, A. Vishwanath, and S. Y. Savrasov, Phys. Rev. B **83**, 205101 (2011).
[11] H. Weng, C. Fang, Z. Fang, B. A. Bernevig, and X. Dai, Phys. Rev. X **5**, 011029 (2015).
[12] A. A. Soluyanov, D. Gresch, Z. Wang, Q. Wu, M. Troyer, X. Dai, and B. A. Bernevig, Nature (London) **527**, 495 (2015).
[13] M. Greiner, P. Carrier, and A. Görling, Phys. Rev. B **81**, 155119 (2010).
[14] N. D. Mermin, Phys. Rev. **137**, A1441 (1965).
[15] M. Städele, J. A. Majewski, P. Vogl, and A. Görling, Phys. Rev. Lett. **79**, 2089 (1997).
[16] M. Städele, M. Moukara, J. A. Majewski, P. Vogl, and A. Görling, Phys. Rev. B **59**, 10031 (1999).
[17] R. T. Sharp and G. K. Horton, Phys. Rev. **90**, 317 (1953).
[18] J. D. Talman and W. F. Shadwick, Phys. Rev. A **14**, 36 (1976).
[19] R. A. Lippert, N. A. Modine, and A. F. Wright, J. Phys. Condens. Matter **18**, 4295 (2006).
[20] See Supplemental Material at http://link.aps.org/supplemental/10.1103/PhysRevLett.120.146401 for LDA band structures of GaBi at low temperatures, LDA and EXX band structures of InBi, the EXX band structure of HgTe at 5 K, LDA band structures of HgTe for various temperatures, and LDA band structures of GaBi, InBi, and HgTe for comparison with literature data.
[21] S. Sharma, J. K. Dewhurst, and C. Ambrosch-Draxl, Phys. Rev. Lett. **95**, 136402 (2005).
[22] M. Betzinger, C. Friedrich, S. Blügel, and A. Görling, Phys. Rev. B **83**, 045105 (2011).
[23] E. Engel, Phys. Rev. B **80**, 161205 (2009).
[24] A. Makmal, R. Armiento, E. Engel, L. Kronik, and S. Kümmel, Phys. Rev. B **80**, 161204 (2009).
[25] X. Chen, X. Hua, J. Hu, J.-M. Langlois, and W. A. Goddard, Phys. Rev. B **53**, 1377 (1996).
[26] S. Biering and P. Schwerdtfeger, J. Chem. Phys. **136**, 034504 (2012).
[27] J. Heyd, E. Scuseria, and M. Ernzerhof, J. Chem. Phys. **118**, 8207 (2003).
[28] S. Chadov, J. Kiss, J. Kübler, and C. Felser, Phys. Status Solidi: Rapid Res. Lett. **7**, 82 (2013).
[29] R. Sakuma, C. Friedrich, T. Miyake, S. Blügel, and F. Aryasetiawan, Phys. Rev. B **84**, 085144 (2011).
[30] A. Svane, N. E. Christensen, M. Cardona, A. N. Chantis, M. van Schilfgaarde, and T. Kotani, Phys. Rev. B **84**, 205205 (2011).
[31] A. Fleszar and W. Hanke, Phys. Rev. B **71**, 045207 (2005).
[32] N. Orlowski, J. Augustin, Z. Gołacki, C. Janowitz, and R. Manzke, Phys. Rev. B **61**, R5058 (2000).
[33] D. J. Chadi, J. P. Walter, M. L. Cohen, Y. Petroff, and M. Balkanski, Phys. Rev. B **5**, 3058 (1972).
[34] W. J. Scouler and G. B. Wright, Phys. Rev. **133**, A736 (1964).
[35] C. Janowitz, N. Orlowski, R. Manzke, and Z. Golacki, J. Alloys Compd. **328**, 84 (2001).
[36] The Magnetization Current Exact-Exchange (MCEXX) code is a pseudopotential plane-wave code developed at the University of Erlangen-Nuremberg.
[37] S. Rohra, E. Engel, and A. Görling, arXiv:cond-mat/0608505.
[38] E. Engel, A. Höck, R. N. Schmid, R. M. Dreizler, and N. Chetty, Phys. Rev. B **64**, 125111 (2001).
[39] *Springer Handbook of Condensed Matter and Materials Data*, edited by W. Martienssen and H. Warlimont (Springer, New York, 2006).
[40] H. Huang, J. Liu, and W. Duan, Phys. Rev. B **90**, 195105 (2014).
[41] J. P. Perdew, K. Burke, and M. Ernzerhof, Phys. Rev. Lett. **77**, 3865 (1996).
[42] I. Lifshitz, Sov. Phys. JETP **11**, 1130 (1960).
[43] G. E. Volovik, Low Temp. Phys. **43**, 47 (2017).
[44] D. Yudin, D. Hirschmeier, H. Hafermann, O. Eriksson, A. I. Lichtenstein, and M. I. Katsnelson, Phys. Rev. Lett. **112**, 070403 (2014).
[45] G. Volovik, JETP Lett. **53**, 222 (1991).
[46] T. Kondo, M. Nakayama, R. Chen, J. Ishikawa, E. Moon, T. Yamamoto, Y. Ota, W. Malaeb, H. Kanai, Y. Nakashima, Y. Ishida, R. Yoshida, H. Yamamoto, M. Matsunami, S. Kimura, N. Inami, K. Ono, H. Kumigashira, S. Nakatsuji, L. Balents, and S. Shin, Nat. Commun. **6**, 10042 (2015).
[47] *Frontiers and Challenges in Warm Dense Matter*, edited by F. Graziani, M. P. Desjarlais, R. Redmer, and S. B. Trickey, Lecture Notes in Computational Science and Engineering Vol. 96 (Springer, New York, 2014).
[48] E.-G. Moon, C. Xu, Y. B. Kim, and L. Balents, Phys. Rev. Lett. **111**, 206401 (2013).
[49] I. F. Herbut and L. Janssen, Phys. Rev. Lett. **113**, 106401 (2014).
[50] L. Janssen and I. F. Herbut, Phys. Rev. B **92**, 045117 (2015).
[51] M. Nakayama, T. Kondo, Z. Tian, J. J. Ishikawa, M. Halim, C. Bareille, W. Malaeb, K. Kuroda, T. Tomita, S. Ideta, K. Tanaka, M. Matsunami, S. Kimura, N. Inami, K. Ono, H. Kumigashira, L. Balents, S. Nakatsuji, and S. Shin, Phys. Rev. Lett. **117**, 056403 (2016).
[52] M. Ferhat and A. Zaoui, Phys. Rev. B **73**, 115107 (2006).
[53] J. W. Nicklas and J. W. Wilkins, Phys. Rev. B **84**, 121308 (2011).
[54] D. C. Langreth and J. P. Perdew, Solid State Commun. **17**, 1425 (1975).
[55] D. C. Langreth and J. P. Perdew, Phys. Rev. B **15**, 2884 (1977).
[56] A. Pribram-Jones, P. E. Grabowski, and K. Burke, Phys. Rev. Lett. **116**, 233001 (2016).
[57] www.eam.uni-erlangen.de.